

High Symbol Rate OFDM Transmission Technologies

F.C. Garcia Gunning¹, S.K. Ibrahim¹, P. Frascella¹, P. Gunning², A.D. Ellis¹

¹Photonic Systems Group, Department of Physics and Tyndall National Institute, University College Cork, Ireland

²Futures Testbed, BT Innovate & Design, Adastral Park, Martlesham Heath, Ipswich IP5 3RE, UK
e-mail: fatima.gunning@tyndall.ie

Abstract: In this paper we discuss high symbol rate all-optical orthogonal frequency division multiplexing (OFDM), focusing on phase optimisation, optimum symbol rate for dispersion managed systems, and Ethernet performance.

©2010 Optical Society of America

OCIS codes: (060.4510) Optical Communications; (060.2360) Fibre Optics Links and Subsystems

1. Introduction

The development of optical OFDM for optical fibre communications [1] has stimulated research in potential applications towards highly spectral efficient networks, whilst maintaining baud rates below 50 Gbaud/s and occupying a narrower bandwidth than other WDM solutions. Capacity/distance products of up to 84.3 Petabit/s-km [2] were achieved recently, as well as information spectral densities (ISD) of 7 bit/s/Hz [3], both using electronic based OFDM (digital OFDM), polarisation division multiplexing (PDM) and coherent detection with off-line processing. With digital OFDM [4], the required orthogonality condition can be easily maintained using matched filters implemented with electronic IFFT/FFT at the transmitter/receiver. Moreover, the electronic circuits can compensate for chromatic dispersion and can be easily scaled-up to higher level modulation formats (QPSK, 8QAM, 16QAM etc) [5]. However, in digital OFDM, the total data rate is constrained by the DSP circuits and the analogue-to-digital and digital-to-analogue converters. Furthermore, in the near term, the successful implementation of digital OFDM for long haul distances will depend on its performance over standard installed systems using dispersion compensation fibres (DCF). So far, such studies have shown that in-line compensation is problematic for digital OFDM [6,7], one of the reasons being the high number of subcarriers, which degrades the non-linear tolerance.

Conversely, in all-optical OFDM [1] and Coherent WDM [8] (analogue OFDM), the implementation of the transmitter and receiver are all-optical, and therefore bandwidth limitations are due to optical components and RF circuitry alone (currently reaching over 100 Gbit/s). Optical integrated devices are maturing, and such systems rely on well known, well-established technologies for their implementation, such as nested Mach-Zehnder modulators, asymmetric Mach-Zehnder filters, array waveguide gratings (AWG), couplers etc, which may require little or no electrical power. In analogue OFDM, a smaller number of optical subcarriers is used in order to achieve high capacity, where each subcarrier has a higher symbol rate, when compared to digital OFDM. Higher level encoding is also possible [9] in all-optical OFDM, especially using integrated devices, and the aggregated capacity could approach Tbit/s scale per laser even without recourse to PDM. Moreover, such systems could be easily implemented within the network by changing the end-terminals only, as performance over standard transmission systems has been shown to be effective, and scales with the subcarrier baud rate, not the total symbol rate [10]. However, the required matched filters at the receiver are harder to achieve [11], and, under non-ideal conditions, phase control of the adjacent optical subcarriers becomes necessary (Coherent WDM). The benefits of using active phase control also extend to pre-compensation of chromatic dispersion [12] and non-linearities [9].

In this paper we will describe the Coherent WDM implementation of all optical OFDM. We will also analyse (a) the requirements for phase optimisation when all subcarriers are independently encoded; (b) the optimum symbol rate for dispersion managed systems; and (c) report the performance of a 0.144 Tbit/s Ethernet superchannel data. In the past we have shown both multi-banded CoWDM [13] (> 1.5Tbit/s of total capacity without PDM) and PDM [14] (0.6 Tbit/s at 2 bit/s/Hz) with negligible penalty.

2. High symbol rate all optical OFDM implementation

All-optical OFDM was demonstrated using two or more subcarriers, spaced at precisely the symbol rate, in order to satisfy the orthogonality condition [6,8]. Figure 1 is a representation of such a system using a single polarisation state. The multi-carrier system is based on the optical generation of subcarriers by a comb generator, implemented, for example, with cascaded Mach-Zehnder modulators [8], by injection locking lasers (ILL) [15], or by recirculating frequency shifters [16]. Each subcarrier can be demultiplexed using an AWG (or ILL), and individually data encoded with an arbitrary modulation format [6,8,15]. Optical phase shifters are used to optimise the relative phase of the optical field between each of the subcarriers to restore the orthogonality for non-ideal receivers (Coherent WDM). In the receiver, the matched filter may be approximated by using cascaded Mach-Zehnders, also

known as optical FFT circuits [11]. Alternatively, AWGs or tuneable bandpass filters may be used for channel selection, and a single asymmetric Mach-Zehnder interferometer (AMZI) to approximate the response of the matched filter. Crosstalk-free channel extraction is completed by signal sampling, either optically [1] or electrically using a receiver with excess bandwidth [8]. Although in this paper we will be presenting results with direct detection, coherent detection has also been demonstrated [6], where the improved optical signal-to-noise ratio (OSNR) tolerance gives a clear advantage for long haul and high ISD systems.

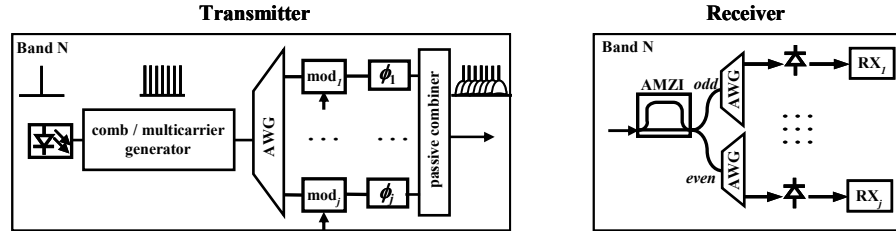


Figure 1: Typical set-up for an analogue OFDM implementation.

Here we are firstly considering the impact of pattern de-correlation and phase control in a Coherent WDM system. In figure 2a we show experimental results for a 31.99 Gbit/s DPSK Coherent WDM system (using injection locking lasers [15]), with three de-correlated and independently DPSK modulated subcarriers (at 10.664 Gbaud/s with PRBS $2^{31}-1$), for optimised and detuned relative phases. Cascaded AMZIs were used to demultiplex and decode the signals, in addition to a tuneable bandpass filter of 30-50 GHz tuneable bandwidth. For the phase-optimised case with bit error rates (BER) above 10^{-4} , all three subcarriers have the same performance, with an average receiver sensitivity (total power) at 10^{-3} of approximately -40.8 dB (OSNR_{0.1nm} \sim 16 dB). However, for lower BER, the centre channel performance deviates from the outer channels by roughly 1 dB at BER of 10^{-9} due to the residual crosstalk from the two non-identical adjacent channels. Note that a smaller penalty is observed if only two data modulators are employed [12]. The penalties are enhanced when the relative phases are detuned. In this case, although the outer subcarriers have identical performances up to BER of $\sim 10^{-8}$ (both have only one subcarrier interfering with its own data); the centre channel performance deteriorates significantly, even for BER of $\sim 10^{-2}$ or 10^{-3} . Therefore, it is clearly evident from these results that, for all optical DPSK OFDM system with more than two subcarriers, phase optimisation significantly improves the system performance.

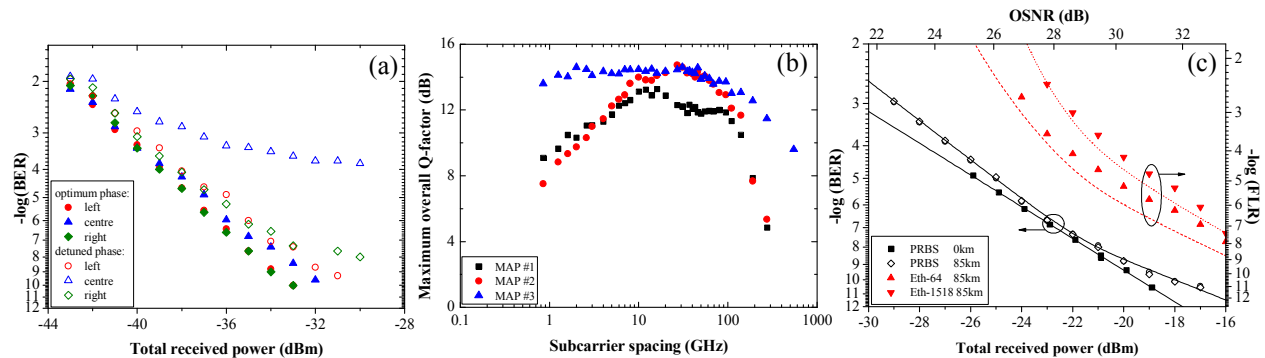


Figure 2: (a) 31.992 Gbit/s DPSK encoded Coherent WDM for optimal and detuned phases. (b) Variations of maximum Q-factor with subcarrier spacing for three dispersion maps. (c) Aggregated Ethernet over Coherent WDM after 85 km SSMF.

Considering now the optimum symbol rate for dispersion managed system, numerical simulations for Coherent WDM were carried out using VPI Transmission Maker v.7.5 (figure 2b). The simulations were performed using j NRZ modulated subcarriers for a range of subcarrier spacings (which were equal to the symbol rate per subcarrier B) for a total capacity of 550 Gbit/s to allow for 1 Tbit/s transmission with PDM. The transmitter was simulated using an array of externally modulated lasers, spaced at precisely the symbol rate and with initial phases of each sub-carrier incremented by $\pi/2$ with respect to its neighbour. The passively multiplexed signals were transmitted over three different links [17], representing respectively an installed inland system, a submarine system, and one without any dispersion compensation. Each link had a length of 2,000 km and an amplifier spacing of 50 km. In all cases, ideal 100% compensation of the accumulated residual dispersion was performed in the optical domain before photo-detection. At the receiver, each channel was demultiplexed by a 3rd order Gaussian filter with a bandwidth equal to 1.8 times the symbol rate followed by a half-bit delay AMZI. The overall estimated Q-factor was obtained by BER averaging of all channels after individual Q-estimation. The overall results of these simulations are shown in Figure 2b which illustrates the variation in Q-factor with channel spacing from 1 GHz (equivalent to 550

OThD1.pdf

subcarriers) to 550 GHz (equivalent to a single carrier). It is evident from figure 2b that current deployed dispersion maps show clear optimum symbol rates, corresponding closely to the data rates for which they were originally designed for (10 Gbit/s for Map #1 and 40 Gbit/s for Map #2).

So far, most of the optical OFDM results are shown with PRBS data, and many assumptions are taken when scaling the results to real Ethernet data streams. In general, one might assume that the loss of one transmitted bit corresponds to the loss of an entire frame, and the distribution of errors is sparse and binomial (no correlated errors). Therefore, the frame loss rate (FLR) and BER can be simply related by equation (1) below, where N is the number of bits in a frame:

$$(1 - \text{FLR}) = (1 - \text{BER})^N \quad (1)$$

Where a given FLR can be inferred from a PRBS measurement. However, unanticipated errors may contribute to divergence from this assumed behaviour [18] and therefore any system that will employ Ethernet standards should ideally be analysed using the particular encoding and scrambling scheme adopted. In order to investigate this issue, we performed transmission experiments of standard 10Gigabit Ethernet LAN-PHY frames using NRZ Coherent WDM at bit rates comparable to the IEEE 802.3ba Ethernet standard effort. A 288 Gbit/s aggregated Ethernet/PRBS Coherent WDM signals was transmitted over 85 km of standard single mode fibre, where each of the seven subcarriers were driven by 41.25 Gbaud/s, obtained by electrically multiplexing two distinct 10.3125 Gbaud/s optical Ethernet streams (frame lengths of 64 and 1518 bytes respectively, generated by a commercial Ethernet testset); and two decorrelated PRBS $2^{31}-1$ signals from a pulse pattern generator (PPG) at the same rate. Synchronisation between PRBS and Ethernet was maintained by feeding a clock signal from the Ethernet testset to the PPG. The 10.000 Gbit/s Ethernet media access layer was characterised by an 8 byte preamble, a frame length of either 64 or 1518 bytes (N at eq. (1) equals 8×64 and 8×1518 respectively) that contained a random payload and an inter-frame gap of 12 bytes. We simultaneously transmitted 1,000,000,000 64-byte and 50,000,000 1518-byte Ethernet frames and analysed the FLR (the “frame length” \times “frame number” products gave roughly equivalent measurement times). Given the number of transmitted frames, we identified frame-loss-free performance a FLR lower than 1×10^{-9} for 64-byte frames and 2×10^{-8} for 1518-byte frames. Figure 2c shows the results for one of the optical subcarriers after transmission. Both PRBS streams have similar performance (closed squares and open circles), and the line represents the fitting of the data. We used this fitting to estimate the FLR accordingly to equation (1), which is plotted with the dotted lines for the two different Ethernet streams. As predicted, the estimates are somewhat optimistic, although no additional error floors were observed. The 288 Gbit/s aggregated Ethernet required a minimum OSNR_{0.1nm} of 32 dB for frame-loss-free performance after 85 km transmission transported over Coherent WDM.

4. Conclusion

In this paper we provided a brief overview of high symbol rate optical OFDM techniques. Phase control between adjacent optical subcarriers is beneficial when non-ideal filters are used, and careful analysis of BER performance below 10^{-4} becomes essential. Moreover, such systems could be readily implemented at the terminals of existing links to enable higher capacities and spectral efficiencies, as performances against common dispersion maps and against Ethernet standards show little degradation of the signal.

The authors would like to thank J. Proudlove from Laser Physics, A. Poustie and J. Reed from CIP for provision on essential lab equipment; and D. Nettet, M. Wilkinson and K. Smith from BT Innovate & Design for very useful discussions. This work is supported by Science Foundation Ireland under Grant 06/IN/1969.

5. References

- [1] H. Sanjoh et al, OFC ThD1 (2002)
- [2] H. Masuda et al, OFC PDP-B5 (2009)
- [3] H. Takahashi et al., OFC PDP-B7 (2009)
- [4] S.L. Jansen et al., ECOC Mo.3.E.3 (2008)
- [5] B.J. Schmidt et al, OFC PDPC3 (2009)
- [6] A. Sano et al., JLT 27 (16) pp. 3705-3713 (2009)
- [7] X. Liu et al., JLT 27 (16) pp. 3632-3640 (2009)
- [8] A.D. Ellis et al., PTL 17 (2) pp. 504-506 (2005)
- [9] F. Inuzuka et al., ECOC 2.3.5 (2009)
- [10] T. Healy et al., ECOC Mo1.3.5 (2007)
- [11] K. Takiguchi et al., OFC OWO3 (2009)
- [12] F.C.Garcia Gunning et al., PTL 18 (12) pp. 1338-1340 (2006)
- [13] F.C.Garcia Gunning et al., ECOC Th4.2.6 (2005)
- [14] F.C.Garcia Gunning et al., CLEO-Europe C18-5-FRI (2007)
- [15] S.K. Ibrahim et al., IEEE Phot. Soc. Annual Meeting ThM1 (2009)
- [16] Y. Ma et al., OFC PDPC1 (2009)
- [17] A.D. Ellis et al., Digest of LEOS Summer Topicals TuD3.2 (2009)
- [18] B. Raahemi, Canadian Conference on Elect. and Comp. Engineering, pp. 412-416 (2005)